Spectral characteristic comparison of rice plants under healthy and water-deficient conditions using Landsat ETM+ data

Landsat 衛星による水稲耕作地への水供給状態の違いによる水稲の分光特性比較研究

I Wayan NUARSA
Faculty of Agriculture, Udayana University

西尾　文彦
Fumihiko NISHIO
Center for Environmental Remote Sensing, Chiba University

本郷　千春
Chiharu HONGO
Center for Environmental Remote Sensing, Chiba University

「写真測量とリモートセンシング」Vol. 50, No. 2, 2011
Journal of the Japan Society of Photogrammetry and Remote Sensing

論文

Spectral characteristic comparison of rice plants under healthy and water-deficient conditions using Landsat ETM+ data

Landsat 衛星による水稲耕作地への水供給状態の違いによる水稲の分光特性比較研究

I Wayan NUARSA, Fumihiko NISHIO and Chiharu HONGO

*I Wayan NUARSA**・西尾　文彦**・本郷　千春**

Abstract : The spectral characteristics of rice plants subject to water deficiency were analysed and compared with healthy rice plants. Under water deficiency conditions, the reflectance of visible bands of the rice plants increased significantly, while the reflectance of near- and middle-infrared bands decreased. For the early detection of water deficiency, the visible band of Landsat ETM+ is more sensitive than the infrared bands. Band-3 showed the highest reflectance differences between rice under water-deficient and healthy conditions. The use of the vegetation index can distinguish rice under water deficiency more clearly than when only using a single band. The Ratio Vegetation Index (RVI) is the best vegetation index for both early detection of water deficiency and distinguishes the two rice conditions.

和文概要：稲作地での水供給状態の違いによる水稲の分光特性を比較した。水供給不足の状況では，水稲からの可視バンドの反射率は著しく増大したが，近赤外及び中間赤外バンドは低下した。水供給が不充分な初期には，Landsat ETM+の可視バンドの反射率は，赤外バンドよりも敏感であった。なかでもバンド3は，水不足と充分な状況では大きな反射率の違いを示した。植生指標（NDVI）は，単バンドの反射率を用いるよりも水供給不足と十分な状態における生育状況を区別することが出来る。稲作指標（RVI）は，初期の水稲作付け状況での水供給状況を検知するために導入し有効であることが明らかになった。

1．Introduction

Rice is the primary food source for more than three billion people and is one of the world's major staple foods. Paddy rice fields account for approximately 15% of the world's arable land (Khush, 2005 ; IRRI, 1993). The growth and yield of rice crops are not only determined by their genetic compositions but are also affected by the environmental factors of their habitats. The progress of a crop is conventionally evaluated by periodical plant samplings, and management practices are guided by the performance in the field (Yang *et al.*, 2008). Nowadays, remote sensing is the preferred technology adopted worldwide for large-scale field monitoring of plant populations, and, through its use, timely and precise site-specific actions may be taken (Bouman, 1995 ; Pierce *et al.*, 1999). If rice crops can be attended to using accurate knowledge of their status in the growth stages, it is possible to respond positively to the supply and demand of varietal growth and production rates.

Vegetation reflectance is a function of optical properties, canopy biophysical attributes, viewing geometry, illumination conditions, and background effects (Asner, 1998 ; Barrett and Curtis, 1992 ; Jacquemoud *et al.*, 1992 ; Myneni *et al.*, 1989). The biophysical attributes of a vegetation crop drive variation in the canopy reflectance characteristics due to the three-dimensional orientation, which provides a better structure and opportunities for photons to interact with multiple surfaces of different plant parts (e.g., leaves, stems), thus favouring

* Faculty of Agriculture, Udayana University

**Center for Environmental Remote Sensing, Chiba University

radiometric reception (Yang and Cheng, 2001; Baret *et al.*, 1994; Jacquemoud, 1993; Kupiec and Curran, 1995; Yang and Su, 2000).

The reflectance of agricultural crops in the visible and infrared regions is currently being used to assess different crop parameters and plant growth status (Carter and Knapp, 2001; Lee *et al.*, 2008; Yang and Chen, 2004). Most green plants exhibit a spectral reflectance profile of a higher reflectance in the near-infrared and a lower reflectance in visible light when grown under normal conditions (Hall *et al.*, 2002). In 'water stress' environments, a reverse fashion is observed due to a decrease in plant vigour and canopy coverage and an increase in the reflectance of chlorophyll absorption (Knipling, 1970; Yang *et al.*, 2007). Crop foliage density and changes in geometry play a key role in the reception of incident radiation and the following biomass formation and accumulation. Variations in crop vegetation, in regular conditions or under stresses, differ greatly in reflectance behaviour, and this may be assessed from the canopy spectral characteristics (Carter and Knapp, 2001; Yang and Chen, 2004).

The monitoring of rice plants using remote sensing data has been widely done. However, the studies have been focused on estimations of rice field areas and production estimations using either optical remote sensing (Bailey *et al.*, 2001; Okamoto and Kawashima, 1999; Fang *et al.*, 1998; Nuarsa *et al.*, 2005; Nuarsa and Nishio, 2007) or radar systems (Shao *et al.*, 2001; Kurosu *et al.*, 1997; Chakraborty *et al.*, 2000; Ribbes and Le Toan, 1999). Investigations of rice plants under abnormal conditions are currently still very limited. Most of them concern the spectral characteristics of rice plants infested by pests and plant diseases (Qin and Zhang, 2005; Yang and Cheng, 2001; Yang *et al.*, 2007), and only a few studies relate to water deficiency (Yang and Su, 2000; Köksal *et al.*, 2008). Studies of the rice plants under abnormal conditions have been done mostly using ground sensing spectroradiometers to acquire the reflectance of rice plants (Yang *et al.*, 2007; Tong *et al.*, 2001). The use of actual remote sensing data of rice plants under abnormal conditions has been limited by difficulties in finding sufficient areas under such conditions (Currey *et al.*, 1987). This study used the actual remote sensing data (Landsat ETM+ images) to monitor the spectral properties of rice plants under water stress. The ground data were obtained from the harvest failure of farms caused by drought (low rainfall) in a broad area of about 421 ha. The objectives of the studies was to analyse differences in the spectral characteristics of rice plants under water stress compared to those under normal conditions using Landsat ETM+ data.

2. Study Area, Data, and Methods

2.1 Background and Study Area

The study area was located in Tabanan Regency, Bali Province, Indonesia, centred at a latitude of 8°31'50" S and a longitude of 115°02'30" E (Fig. 1). The Tabanan Regency was selected for the study area due to Tabanan being the central production area of rice in Bali. In the study area, the rice

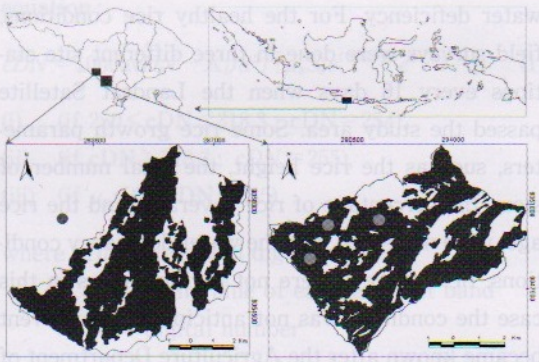

a b

Fig. 1 Location map of the study area. The black colour indicates rice field areas, and the white colour indicates other land use areas. Left below (a) is the study area for the rice under water deficiency. The green point next to the study area is the nearest rainfall station used to obtain a rainfall data. Right below (b) is the study area for the rice under healthy conditions. The three orange points in that image are the ground sites where the field measurement was done.

planting is organised by a *subak*. The *subak* is the farmer's social organisation that manages the irrigation water. Each subak controls around 150−300 ha of rice fields (Food Crops Agriculture Department, 2006). They usually plant rice at the same times. An advantage for the remote sensing study with this farming system is that the monitoring is made easier due to the availability of a wide rice area.

Because irrigation water is a constraining factor in the study area, rice planting is done in turns between the *Subaks*. Alternative plants to rice plants include session agriculture crops such as corn, soybeans, etc. The length of the growth cycle of rice can vary from three to six months for different varieties (Casanova, 1998). In the study area, the average length of the growth cycle of rice is 115 days, with production reaching 5.0 tons/ha (Food Crops Agriculture Department, 2006). In one year, the farmer usually plants rice twice in two planting sessions.

This study was carried out on two different sites and during two planting sessions. One experimental session was conducted under healthy rice conditions, and the other session was conducted under water deficiency. For the healthy rice conditions, field surveys were done in three different site stations every 16 days when the Landsat Satellite passed the study area. Some rice growth parameters, such as the rice height, the total number of stem, the percentage of rice coverage, and the rice age, were measured. For the water deficiency conditions, field surveys were not performed, as in this case the condition was not anticipated. This event became known after the Agriculture Department of the local government released relevant reports. However, the locations and planting dates of these areas were precisely recognised. Hence, the investigation of rice under healthy and water deficiency conditions could evidently be done successfully.

According to the Agriculture Department of the local government, the cause of the occurrence of drought was that the planting of rice was done outside the normal planting season. The farmers had speculated on rain coming soon after planting. Unfortunately, the rainfall had not begun from the rice age of 15 days after planting until one month after (Table 1). This situation caused around 421 ha of rice plants in the study area to experience a

Table 1 Monthly rainfall of the nearest rainfall station from the study area (BMG, 2006)

Month	Rainfall (mm)
January	322
February	183
March	295
April	138
May	0
June	27
July	106
August	14
September	76
October	214
November	53
December	391

The zero value of rainfall in May indicated that the rainfall in that month was less than 1 mm. Planting was done on 15 April 2005. Beginning from May, the rice plants did not get water, and in June the rainfall was very low. This condition caused the rice to experience drought.

Table 2 Site characteristics of rice under healthy and water-deficient conditions

Parameters	Healthy rice	Water-deficient rice
Soil type	Latosol/Vertisol	Latosol/Vertisol
Land slope (%)	0-15	0-8
Elevation (m above sea level)	38-52	5-15
(Fertiliser and pesticide used)	Agriculture Department recommendation	Agriculture Department recommendation
Water source	Permanent irrigation	Rainfall
Rice variety	Ciherang	Ciherang
Peak of Transplanting	12 June 2005	15 April 2005
Average temperature in planting session (°C)	25.7	26.1
Average duration of solar radiation in planting session (%)	75	79

drought. The rice production under these circumstances was approximately 0.35 ton/ha of grain dry weight (less than 6% of normal condition) (Food Crops Agriculture Department, 2006).

The site characteristics of the rice under healthy and water-deficient conditions during the rice growing circle were the same for the soil type and rice variety and were similar for the land slope, elevation, average temperature, average duration of solar radiation as well as fertiliser and pesticide treatment. However, the water resources for the rice field irrigation were different (Table 2). In the healthy rice area, water was mainly derived from the permanent irrigation water. On the other hand, for rice in water-deficient sites, water comes solely from rainfall. The permanent irrigation water guarantees the availability of water and the sustainability of healthy rice crops more than rainfall can. The peak of transplanting was done on 12 June 2005 at healthy rice and 15 April 2005 at Water-deficient rice.

2.2 Landsat Image Data

Landsat satellite images had eight bands including thermal and panchromatic bands. In the visible, near-infrared, and middle-infrared regions, Landsat ETM+ had a 30-m spatial resolution. However, in the thermal and panchromatic regions, the spatial resolutions were 60 m and 15 m, respectively. This study used visible and reflectance infrared bands (Bands 1-5 and Band 7) of Landsat ETM+. Although the Landsat ETM+ used in this study has a scan-line corrector (SLC) off, the better spatial, spectral, and temporal resolution of its images caused it to still be relevant for use. With the 16 days of temporal resolution, Landsat ETM+ is the ideal satellite image for rice monitoring seeing as rice has only a 115-day cycle from planting to harvest. These images can be downloaded at USGS Global Visualization Viewer (http://glovis.usgs.gov).

Because the length of the rice growth cycle is around 115 days and the temporal resolution of Landsat ETM+ images is 16 days, the total of the time series images that can be collected in one rice growth cycle is around six images for different acquisition dates. Some of the images cannot be used, due to cloud conditions or the appearance of gap values in the SLC-off mode of the station points. This caused a reduced availability of images. Fortunately, this study area was covered by two scenes of Landsat images in different paths. The total of the Landsat images used in this study is shown in Tables 3 and 4 for rice in sites with healthy and water-deficient conditions, respectively.

2.3 Data analysis

2.3.1 Radiometric corrections

In the temporal analysis of remote sensing data, radiometric corrections are an important part of the image analysis. The digital number (DN) of the Landsat ETM+ at different acquisition dates should be converted to the corrected digital number (cDN) to eliminate the radiometric and atmospheric effects, so that they have comparable values. In this study, we used the simple radiometric correction model introduced by Pons and Solé-Sugrañes (1994). The formula of this model is shown in the following equation :

$$cDN = 1000\mathrm{a}(DN - K_l)d^2/[\mu_s S_0 e^{(-\tau_0/\mu_0)} e^{(-\tau_0/\mu_v)}], \quad (1)$$

(i) (if $250 < \mathrm{cDN} \leq 318.3$; $\mathrm{cDN} = 254$),

(ii) (if $\mathrm{cDN} > 318.3$; $cDN = 255$),

(iii) (if $\mu_s \leq 0$; $\mathrm{cDN} = 255$),

where cDN = corrected digital number
a = gain value of each Landsat band
DN = digital number
K_l = radiances value of zone totally in shade
d = actual Sun-Earth distance
μ_s = cosine of the incident angle
S_0 = exoatmospheric solar irradiance
τ_0 = optical depth of the atmosphere
μ_0 = cosine of the solar zenith angle
μ_v = cosine of sensor view angle

cDN is the corrected digital number and the conver-

Table 3 Values of d (1), μ_0(2), and K_1(3) for every acquisition date of Landsat ETM+ in healthy rice

Acquisition date	Path	Row	DOY	d	μ_0	K_1					
						ETM1	ETM2	ETM3	ETM4	ETM5	ETM7
26 April 2002	116	66	116	1.00626	0.79414	51	31	23	20	17	11
21 May 2002	116	66	141	1.01210	0.75100	53	32	22	23	19	14
7 July 2005	117	66	188	1.01669	0.71514	52	34	22	25	21	11
1 August 2005	116	66	213	1.01497	0.74624	50	31	23	19	16	12
17 August 2005	116	66	229	1.01244	0.78085	53	33	23	22	18	13
24 August 2005	117	66	236	1.01103	0.80312	55	35	24	23	15	10
4 October 2005	116	66	277	1.00033	0.88006	54	34	24	21	17	12
12 November 2005	117	66	316	0.98983	0.90081	52	31	22	24	21	11

Sources: (1) Chander *et al.* (2009); (2) our image with calculations; (3) the DN of our image. DOY is the day of year.

Table 4 Values of d (1), μ_0(2), and K_1(3) for every acquisition date of Landsat ETM+ in water-deficient rice

Acquisition date	Path	Row	DOY	d	μ_0	K_1					
						ETM1	ETM2	ETM3	ETM4	ETM5	ETM7
18 April 2005	117	66	108	1.00409	0.80647	52	33	23	18	15	11
27 April 2005	116	66	117	1.00653	0.79287	52	31	23	23	18	15
13 May 2005	116	66	133	1.01043	0.76522	56	34	23	22	17	12
20 May 2005	117	66	140	1.01191	0.75302	48	30	22	18	15	12
29 May 2005	116	66	149	1.01355	0.73857	54	34	23	22	18	12
21 June 2005	117	66	172	1.01625	0.71480	62	41	25	23	13	9
30 June 2005	116	66	181	1.01665	0.71309	57	36	27	21	18	12
23 July 2005	117	66	204	1.01592	0.72621	51	33	23	24	22	12

Sources: (1) Chander *et al.* (2009); (2) our image with calculations; (3) the DN of our image. DOY is the day of year.

Table 5 Values of τ_0(1), S_0(2), and a (3) for every spectral Landsat Band for both healthy and water-deficient rice

Band	τ_0	S_0 ($Wm^{-2}\mu m^{-1}$)	a
ETM1	0.5	1997	0.7757
ETM2	0.3	1812	0.7957
ETM3	0.25	1533	0.6192
ETM4	0.20	1039	0.9655
ETM5	0.125	230.8	0.1257
ETM7	0.075	84.9	0.0437

Sources: (1) Dozier (1989); (2) Chander *et al.* (2009); (3) our image with calculations.

sion of the effective reflectance to the common 8-bit format of most image processors. The range of the output values has been limited to between 0 and 255. Note that a, K_1, S_0, and τ_0 depend on the wavelength and have different values for each spectral band; K_1 varies for each image because it is related to and depends on atmospheric conditions; μ_0 and μ_s depend on the latitude, date, and time of the satellite pass; besides that, μ_s also depends on the slope and aspect of each pixel; d depends on the date of the satellite pass, and μ_v depends on the sensor viewing angle. The parameter μ_v is 1 in most Landsat images because v is 0 at the nadir and has small values on the rest of the images (Pons and Solé-Sugrañes, 1994). The parameters needed in the study to calculate cDN are shown in Tables 3-5.

Practically, to apply the algorithm above we only need a DEM of enough quality (altimetrically and planimetrically) because all of the other parameters are known (e.g., S_0) or can be inferred from images (e.g., K_1). To avoid overcorrections and undercorrections on the ridges and channels and to account for local phenomena, it is important to use a DEM with a planimetric resolution comparable to the geometric resolution of the image. Naugle and Lashlee (1992) showed that a DEM of 95 m can be insufficient for a Landsat TM image over rugged terrain. In this study, we derived a DEM from the topographical map with a spatial resolution of 30 m.

Table 6 Several vegetation indexes used in the study for identifying the spectral characteristics of rice in healthy and water-deficient conditions

No	Vegetation Index	Formula
1	Normalised Difference Vegetation Index (NDVI)	$NDVI=\frac{nir-r}{nir+r}$
2	Ratio Vegetation Index (RVI)	$RVI=\frac{nir}{r}$
3	Infrared Percentage Vegetation Index (IPVI)	$IPVI=\frac{nir}{nir+r}$
4	Difference Vegetation Index (DVI)	$DVI=nir-r$
5	Transformed Vegetation Index (TVI)	$TVI=\frac{100}{\sqrt{\frac{nir-r}{nir+r}+0.5}}$
6	Soil-Adjusted Vegetation Index (SAVI)	$SAVI=\frac{(1+L)(nir-r)}{nir+r+L}$
7	Normalised Difference Water Index (NDWI-1)	$NDWI1=\frac{nir-swir1}{nir+swir1}$
8	Normalised Difference Water Index (NDWI-2)	$NDWI2=\frac{nir-swir2}{nir+swir2}$

Here, nir, r, swr1, swr2, and L are the near-infrared band, red band, middle-infrared (Band-5 of Landsat ETM+), middle-infrared (Band-7 of Landsat ETM+), and canopy background brightness correction factor, respectively.

2.3.2 Spectral Characteristic Analysis of Rice Plants

Gathering reflectance values from the Landsat pixels for both rice conditions over the entire time period of rice growth was the next step of the data analysis. In each image of an acquisition date, a 200-pixel sample was taken randomly in the field observation site at both healthy and water-deficient sites (Fig. 1). The average value of the sample was used as a representative of the spectral value of that acquisition date. Based on the spectral value, the vegetation index was calculated. Several vegetation indexes that were evaluated in the study are shown in Table 6.

Based on the spectral and vegetation index values, spectral analysis was performed by means of comparing the values for rice under healthy and water-deficient conditions, using statistical analysis (paired-samples T test).

3. Results and Discussion

3.1 Rice growth parameters under healthy condition

Based on field survey data and statistical analysis of rice under healthy condition, there was a quadratic relationship between some of rice growth parameters (rice height and stem total) and rice age. However, percentage of rice coverage was better expressed by a linear relationship with rice age. Rice coverage height showed the best relationship with the rice age, followed by rice height and stem

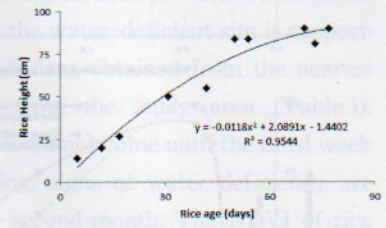

a

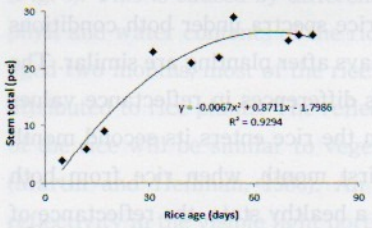

b

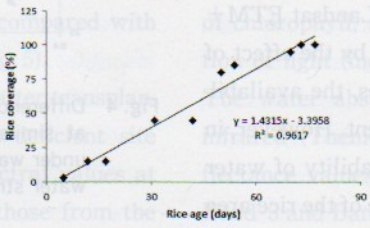

c

Fig. 2 Relationship between rice height (a), stem total (b) and rice coverage (c) with rice age.

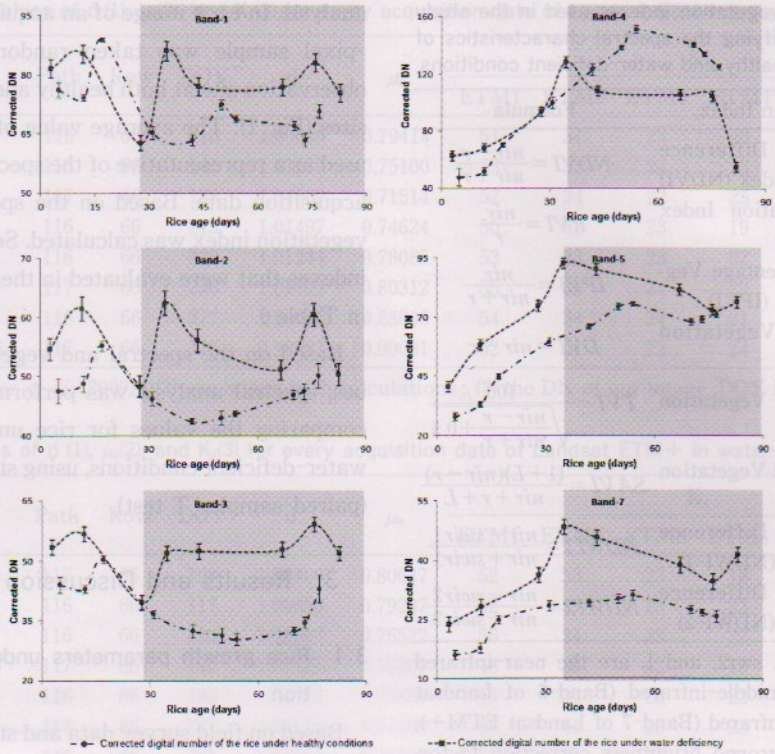

Fig. 3 Spectral characteristic of rice under healthy and water-deficient conditions for all reflective bands of Landsat ETM+. The white areas in the chart indicate that both reflectances of the rice have similar forms, while the dark areas show different forms of rice reflectance.

total with the R^2 value were 0.9617, 0.9544, and 0.9294 respectively (Fig. 2a, Fig. 2b, and Fig. 2c).

3.2 Spectral characteristics of rice under healthy and water-deficient conditions

The trends of rice spectra under both conditions for rice aged 30 days after planting are similar. The tendency towards differences in reflectance values is only seen when the rice enters its second month (Fig. 3). In the first month, when rice from both conditions are in a healthy state, the reflectance of rice under water deficiency appears higher than that in healthy condition sites for most Landsat ETM+ bands (Fig. 4). This result is caused by the effect of water coverage. In healthy rice sites, the availability of water for irrigation is sufficient. However, in water-deficient rice sites, the availability of water is limited. Therefore, the reflectance of the rice area for healthy rice sites is controlled by the water, whereas in water-deficient sites, the reflectance is

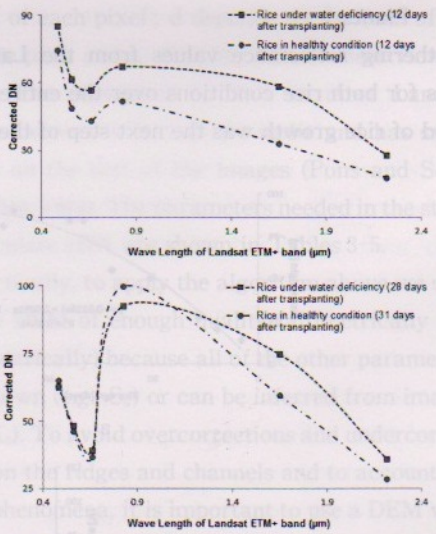

Fig. 4 Differences of the spectral characteristics of rice at similar ages at times when the rice plants under water deficiency did not yet show signs of water stress.

influenced by the moist soil surface. Moist soil has a higher reflectance than water in the visible, near

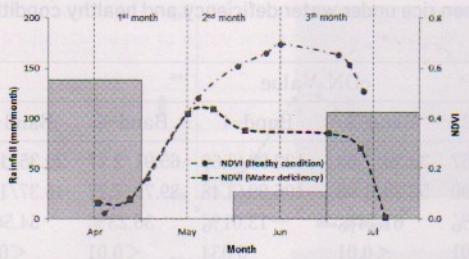

Fig. 5 The total monthly rainfall in water-deficient sites beginning from the plantation time through the next three months. Rice was transplanted in the middle of April. Starting from a rice age of two weeks, there was no rain at all until the next month. Rainfall in small amounts occurred at a rice age of seven weeks. The chart also illustrates the relationship between monthly rainfall and periods of water stress (see the dashed line). The connected line just shows a comparison of the rice under normal conditions in the same rice age (it does not the actual of rice planting).

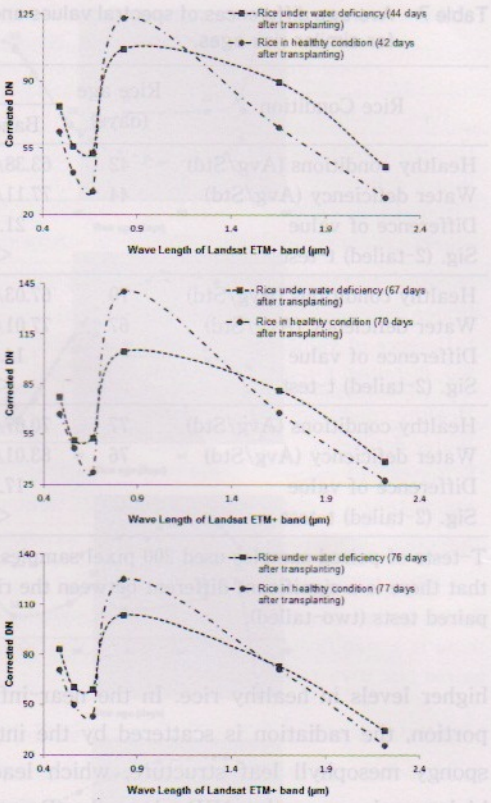

Fig. 6 Differences of the spectral characteristics of rice at similar ages at times when the rice plants in water deficiency did show signs of water stress. The third comparisons were done for rice ages greater than one month.

-infrared and middle-infrared regions of the electromagnetic spectrum (Harrison and Jupp, 1989).

In the second month, the trend of spectral changes for the rice became inverted. Under normal conditions, when the rice enters the second month, the reflectance values of Band-1, Band-2, and Band-3 should decrease, while in Band-4, Band-5, and Band-7 they should increase. However, at the water-deficient site, the reverse occurs (see Fig. 3 in the dark area). This result shows that there has been water stress. The appearance of water stress in the second month in the water-deficient site is supported by the rainfall data obtained from the nearest rainfall station from the study area (Table 1). Although the rain did not come until the third week after rice planting, signs of water deficiency are only seen in the second month. The NDVI of rice under water deficiency decreased significantly in the beginning of the second month compared with the rice under normal conditions (Fig. 5).

Beginning from the second month after transplantation, when the rice in the water-deficient site shows signs of water stress, the spectral values at all Landsat bands are higher than those from the healthy rice, except for Band-4 (Fig. 3). The maximum difference was seen for rice that was around two months (67−70 days after plantation time) old (Fig. 6). This is caused by differences in the chlorophyll and water contents of the rice plants. On rice aged two months, most of the rice area coverage is attributed to rice plants. The reflectance properties of the rice will be similar to vegetation in general (Martin and Heilman, 1986). An increase in leaf reflectivity in the visible light portion as a response to water stress is caused by the metabolic sensitivity of chlorophyll, resulting in a less efficient absorption of light (increased reflection) (Knipling, 1970). The water absorption properties of the middle-infrared (Thenkabail *et al.*, 1994b) cause the reflectance values of rice under water deficiency in Band-5 and Band-7 of Landsat ETM+ to be higher than those of healthy rice. However, in Band-4, the chlorophyll pigments that are present in leaves have

Table 7 Average differences of spectral values and t-tests between rice under water deficiency and healthy conditions for similar rice ages.

Rice Condition	Rice age (days)	cDN Value					
		Band-1	Band-2	Band-3	Band-4	Band-5	Band-7
Healthy conditions (Avg/Std)	42	63.38/1.91	42.28/1.67	32.39/1.63	122.99/3.60	65.91/2.27	29.35/1.93
Water deficiency (Avg/Std)	44	77.11/2.15	56.03/1.90	52.38/1.93	106.99/3.48	89.79/2.27	45.37/1.93
Difference of value		21.65%	32.52%	61.74%	−13.01%	36.23%	54.56%
Sig. (2-tailed) t-test		<0.01	<0.01	<0.01	0.034	<0.01	<0.01
Healthy conditions (Avg/Std)	70	67.03/1.96	46.80/1.73	32.39/1.63	140.28/3.71	68.04/2.27	27.57/1.93
Water deficiency (Avg/Std)	67	77.01/2.02	51.08/1.70	52.79/1.92	104.51/3.55	81.36/2.31	38.50/1.95
Difference of value		14.90%	9.14%	62.99%	−25.50%	19.58%	39.67%
Sig. (2-tailed) t-test		<0.01	<0.01	<0.01	<0.01	<0.01	<0.01
Healthy conditions (Avg/Std)	77	70.67/1.96	50.03/1.73	42.95/1.63	125.15/3.71	71.23/2.27	25.78/1.93
Water deficiency (Avg/Std)	76	83.01/2.19	60.38/1.92	59.29/1.92	103.71/3.60	73.04/2.29	34.46/1.95
Difference of value		17.46%	20.69%	38.04%	−17.13%	2.55%	33.67%
Sig. (2-tailed) t-test		<0.01	<0.01	<0.01	0.038	<0.01	<0.01

T-tests of paired samples used 200 pixel samples. A value less than 0.05 in the T-tests of paired samples indicates that there is a significant different between the rice under water deficiency and healthy conditions for two-sample paired tests (two-tailed).

higher levels in healthy rice. In the near-infrared portion, the radiation is scattered by the internal spongy mesophyll leaf structure, which leads to higher values on the NIR channels (Baret and Guyot, 1991). Therefore, the reflectance of Band-4 in healthy rice is higher than that of water-deficient rice (Fig. 3).

For the early detection of water deficiency, the visible band (Bands 1-3) is more sensitive than near- and middle-infrared bands of Landsat ETM+. In the visible band, the changing trend of reflectance values was detected at the beginning of the third observation (before rice is one month old); in near- and middle-infrared, however, it was just detected at the fourth observation (rice aged more than one month) (Fig. 3). This means that the visible band is more sensitive for early water deficiency detection than the near- and middle-infrared bands of Landsat ETM+. The highest percentage difference of values of Landsat ETM+ bands between healthy rice and water-deficient rice at similar rice ages was shown by Band-3 (Table 7).

The comparison by means of statistical tests (t-test) showed that the entire Landsat ETM+ bands evaluated in this study (B1-B5 and B7) for similar rice ages provided a significant distinction of spectra between rice under water deficiency and healthy conditions (Sig.<0.05) in a two-tailed t-test (Table 7). It means that rice field spectral in water deficiency and healthy was different statistically.

3.2 Vegetation index of healthy and water-deficient rice

Using multiple bands of Landsat ETM+ in the form of a vegetation index delivers a clearer distinction between rice under healthy and water-deficient conditions than when using a single band. Fig. 7 shows that in the first month after plant time, the vegetation index has a similar pattern due to both rice still being under normal conditions. However, when the rice plants under water deficiency enter the second month of growth, when there is a period of water stress, the difference in the vegetation index for the two rice conditions is high for all vegetation indexes evaluated in this study. All vegetation index values for the water-deficient rice are significantly lower than those for the healthy rice, except for the TVI. The distinction of TVI trends compared with other vegetation indexes is because the TVI equation is in a reverse form from other

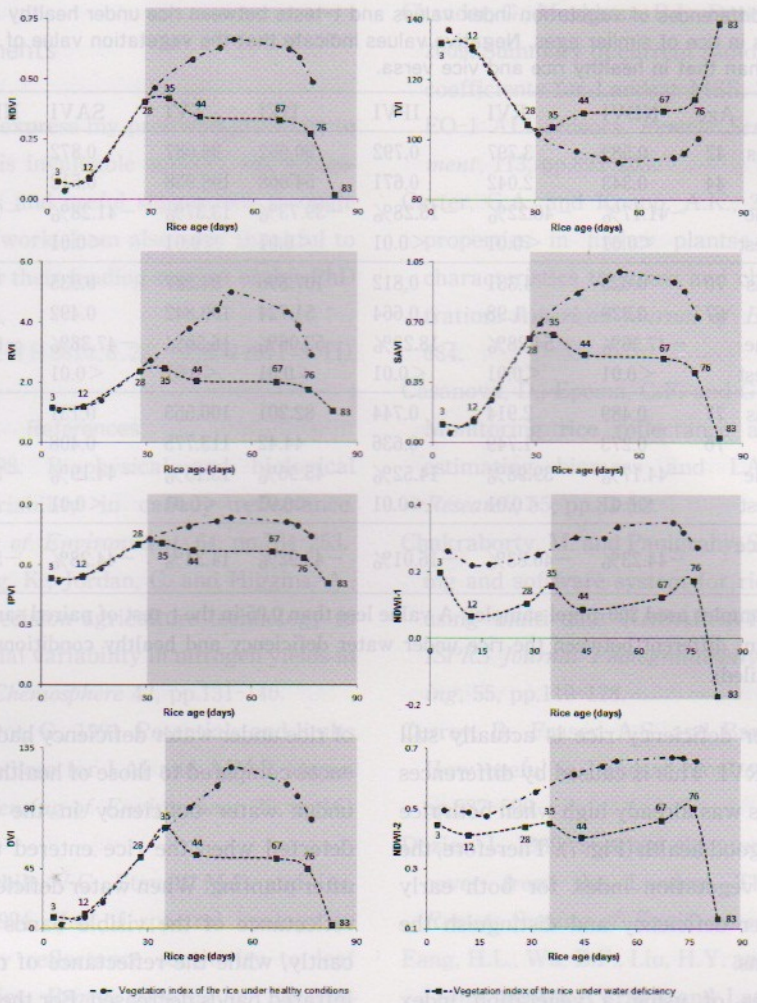

Fig. 7 Vegetation index comparison of rice under healthy and water-deficient conditions. Eight vegetation indexes were evaluated, including NDVI, TVI, RVI, DVI, SAVI, IPVI, NDWI-1, and NDWI-2. The white areas in the chart indicate that both rice are still under normal conditions, while the dark areas show rice plants experiencing water deficiency.

vegetation index equations (Table 6).

For three observations of the vegetation index for similar rice ages, NDWI-1 provides the highest distinction between two rice conditions at rice ages of 42-44 days and 67-70 days, at −71.19% and −63.98%, while for rice ages of 76-77 days the highest difference of a vegetation index value is given by DVI with the value of −45.96% (Table 8). The highest difference average is provided by NDWI-1 with the value of −57.36% followed by RVI, SAVI and NDVI. However, for the early detection of water deficiency, the NDVI, RVI, and SAVI provided better responses. They could detect rice under water stress after the third observation (after rice age of 28 days). Other vegetation indices provided response after the fourth observation (after rice age of 35 days). A high distinction of vegetation index between rice under healthy conditions and in water stress was also shown by the statistical test (t-test). The entire vegetation index provided a significant difference between two rice conditions, with significant values in two-tailed t-tests lower than 0.05 (Table 8). Although NDWI-1 provided the highest difference average between two rice conditions compared with other vegetation index, the differences of NDWI-1 value between

Table 8 Average differences of vegetation index values and t-tests between rice under healthy and water-deficient conditions in rice of similar ages. Negative values indicate that the vegetation value of water-deficient rice is lower than that in healthy rice and vice versa.

Rice Condition	Age	NDVI	RVI	IPVI	DVI	TVI	SAVI	NDWI-1	NDWI-2
Healthy conditions	42	0.583	3.797	0.792	90.602	96.087	0.872	0.302	0.615
Water deficiency	44	0.343	2.042	0.671	54.608	108.938	0.512	0.087	0.404
Difference of value		−41.17%	−46.22%	−15.28%	−39.73%	13.37%	−41.28%	−71.19%	−34.31%
Sig. (2-tailed) t-test		<0.01	<0.01	<0.01	<0.01	<0.01	<0.01	<0.01	<0.01
Healthy conditions	70	0.625	4.331	0.812	107.896	94.287	0.935	0.347	0.672
Water deficiency	67	0.329	1.98	0.664	51.724	109.842	0.492	0.125	0.462
Difference of value		−47.36%	−54.28%	−18.23%	−52.06%	16.50%	−47.38%	−63.98%	−31.25%
Sig. (2-tailed) t-test		<0.01	<0.01	<0.01	<0.01	<0.01	<0.01	<0.01	<0.01
Healthy conditions	77	0.489	2.914	0.744	82.201	100.555	0.731	0.275	0.658
Water deficiency	76	0.273	1.749	0.636	44.42	113.775	0.408	0.174	0.501
Difference of value		−44.17%	−39.98%	−14.52%	−45.96%	13.15%	−44.19%	−36.90%	−23.86%
Sig. (2 tailed) t-test		<0.01	<0.01	<0.01	<0.01	<0.01	<0.01	<0.01	<0.01
Average difference values		−44.23%	−46.83%	−16.01%	−45.92%	14.34%	−44.28%	−56.78%	−29.81%

T-tests of paired samples used 200-pixel samples. A value less than 0.05 in the t-test of paired samples indicates that there is a significant different between the rice under water deficiency and healthy conditions for a two-sample paired test (two-tailed).

healthy and water deficiency rice is actually still smaller than the RVI. This is caused by differences of NDWI-1 values was already high when both rice plants are still in good health (Fig. 7). Therefore, the RVI is the best vegetation index for both early detection of water deficiency and distinguish the two rice conditions.

The advantages of using a vegetation index compared with a single band is to reduce the spectral data to a single number that is related to the physical characteristics of vegetation (e.g., leaf area, biomass, productivity, photosynthetic activity, or percent cover) (Baret and Guyot, 1991 ; Huete, 1988) while minimising the effects of internal (e.g., canopy geometry and leaf and soil properties) and external (e.g., sun-target-sensor angles and atmospheric conditions at the time of image acquisition) factors on the spectral data (Baret and Guyot, 1991 ; Huete and Warrick 1990 ; Huete and Escadafal, 1991).

4 . Conclusions

Corrected digital number and vegetation indices of rice under water deficiency had significant differences compared to those of healthy rice. Rice plants under water deficiency in the study area were detected when the rice entered the second month after planting. When water deficiency happened, the reflectance of the visible bands increased significantly, while the reflectance of near- and middle-infrared bands decreased. For the early detection of water stress, the visible band was more sensitive than the near- and middle-infrared bands. The red band (B3) of Landsat ETM+ was the best band to distinguish rice plants under water stress and healthy conditions because it provided the highest difference in the reflectance percentage between rice under healthy and water-deficient conditions. The utilisation of the vegetation index to discriminate between rice under healthy and water-deficient conditions provided better results than when using a single band. The RVI is the best vegetation index for both early detection of water deficiency and distinguish the two rice conditions. Although Landsat ETM+ had SLC-off, it can still be used for rice monitoring because it has good spatial, spectral, and temporal resolutions, especially for session plants.

Acknowledgments

I would like to express my profound gratitude to my advisor for his invaluable support, encouragement, supervision, and useful suggestions throughout this research work. I am also very thankful to JSPS Ronpaku for their funding support of this PhD research program.

(受付日2010.8.23, 受理日2011.3.11)

References

Asner, G.P., 1998. Biophysical and biological sources of variability in canopy reflectance. *Remote Sensing of Environment*, 64, pp.234-253.

Bailey, J.S., Wang, K., Jordan, C. and Higgins, A., 2001. Use of precision agriculture technology to investigate spatial variability in nitrogen yields in cut grassland. *Chemosphere* 42, pp.131-140.

Baret, F. and Guyot, G., 1991. Potentials and limits of vegetation indices for LAI and APAR assessment. *Remote Sensing of Environment*, 35, pp.161-173.

Baret, F., Vanderbilt, V.C., Steven, M.D. and Jacquemoud, S., 1994. Use of spectral analogy to evaluate canopy reflectance sensitivity to leaf optical properties. *Remote Sensing of Environment*, 48, pp.253-260.

Barrett, E.C. and Curtis, L.F., 1992. Introduction to environmental remote sensing. In: *Introduction to Environmental Remote Sensing*, 3, p.426 (Barrett, E.C. and Curtis, L.F., Eds.), Chapman & Hall, London, U.K.

Bouman, B.A.M., 1995. Crop modeling and remote sensing for yield prediction. *Netherlands Journal of Agricultural Science*, 43, pp.143-161.

Food Crops Agriculture Department, 2006. *Annual report of food crops*. Department Agriculture of Local Government, Bali Province Indonesia, 3, 125-130.

BMG, 2006. *Report of Monthly Rainfall*. Meteorological and Geophysical Agency, 2, pp.45-50 (Bali Province, Indonesia).

Chander, G., Markham, B.L., Dennis L. Helder, D.L., 2009. Summary of current radiometric calibration coefficients for Landsat MSS, TM, ETM+, and EO-1 ALI sensors. *Remote Sensing of Environment*, 113, pp.893-903.

Carter, G.A. and Knapp, A.K., 2001. Leaf optical properties in higher plants: Linking spectral characteristics to stress and chlorophyll concentration. *American Journal of Botany*, 88, pp.677-684.

Casanova, D., Epema, G.F. and Goudriaan, J., 1998. Monitoring rice reflectance at field level for estimating biomass and LAI. *Field Crops Research*, 55, pp.83-92.

Chakraborty, M. and Panigrahy, S., 2000. A Processing and software system for rice crop inventory using multi-date RADARSAT ScanSAR data. *ISPRS Journal Photogrammetry and emote Sensing*, 55, pp.119-128.

Currey, B., Fraser, A.S. and Bardsley, K.L., 1987. How useful is Landsat monitoring. *Nature*, 328, pp.587-590.

Dozier, J., 1989. Spectral signature of Alpine snow cover from the Landsat Thematic Mapper, *Remote Sensing of Environment*, 28, pp.9-22.

Fang, H.L., Wu, B.F., Liu, H.Y. and Huang, X., 1998. Using NOAA AVHRR and Landsat TM to estimate rice area year-by-year. *International Journal of Remote Sensing*, 19, pp.521-525.

Food Crops Agriculture Department, 2006. *Annual report of food crops*, 3 pp.125-130 (Department Agriculture of Local Government, Bali Province Indonesia).

Gausman, H.W., 1974. Leaf reflectance of near-infrared. *Photogrammetric Engineering and Remote Sensing*, 40, pp.183-191.

Hall, A., Lamb D.W., Holzapfel, B. and Louis J., 2002. Optical remote sensing applications for viticulture—a review. *Australian Journal of Grape and Wine Ressearch*, 8, pp.36-47.

Harrison, B.A. and Jupp, D.L.B., 1989. *Introduction to remotely sensed data*, 1, p.65 (CSIRO Publications).

Huete, A.R. and Escadafal, R., 1991. Assessment of biophysical soil properties through spectral decomposition techniques. *Remote Sensing of Environment*, 35, pp.149-159.

Huete, A.R. and Warrick, A.W., 1990. Assessment of vegetation and soil water regimes in partial canopies with optical remotely sensed data. *Remote Sensing of Environment*, 32, pp.115-167.

Huete, A.R., 1988. A soil-adjusted vegetation index (SAVI). *Remote Sensing of Environment*, 25, pp. 295-309.

IRRI, 1993. 1993-1995 *IRRI Rice Almanac*. Manila : International Rice Research Institute.

Jacquemoud, S., 1993. Inversion of the PROSPECT+SAIL canopy reflectance model from AVIRIS equivalent spectra : theorectical study. *Remote Sensing of Environment*, 44, pp.281-292.

Jacquemoud, S., Baret, F. and Hanocq, J.F., 1992. Modeling spectral and bidirectional soil reflectance. *Remote Sensing of Environment*, 41, pp.123-132.

Khush, G.S. 2005. What it will take to feed 5 billion rice consumers in 2030. *Plant Molecular Biology*, 59, pp.1-6.

Knipling, E.B., 1970. Physical and physiological basis for the reflectance of visible and near-infrared radiation from vegetation. *Remote Sensing of Environment*, 1, pp.155-159.

Köksal, E.S., Kara, T., Apan, M., Üstün, H. and İlbeyi, A., 2008. Estimation of green bean yield, water deficiency and productivity using spectral indexes during the growing season. *Irrigation and Drainage Systems*, 22, pp.209-223.

Kupiec, J.A. and Curran, P.J., 1995. Decoupling effects of the canopy and foliar biochemicals in AVIRIS spectra. *International Journal of Remote Sensing*, 16, pp.1731-1379.

Kuroso, T., Fujita, M. and Chiba, K., 1997. Monitoring of rice fields using multi-temporal ERS-1 C-band SAR data. *International Journal of Remote Sensing*, 18, pp.2953-2965.

Lee, Y.-J., Yang, C.-M., Chang, K.-W. and Shen Y., 2008. A simple spectral index using reflectance of 735 nm to assess nitrogen status of rice canopy. *Agronomy Journal*, 100, pp.205-212.

Lillesand, T.M. and Kiefer, R.W., 1994. *Remote Sensing and Image Interpretation*, 3, pp.427-517 (New York : John Wiley and Sons).

Martin, R.D.J. and Heilman, J.L., 1986. Spectral reflectance patterns of flooded rice. *Photogrammetric Engineering and Remote Sensing*, 52, pp. 1885-1890.

Myneni, R.B., Ross, J. and Asrar, G., 1989. A review on the theory of photon transport in leaf canopies. *Agricultural and Forest Meteorology*, 45, pp.1-153.

Naugle, B.I. and Lashlee, J.D., 1992. Alleviating topographic influences on land-cover classifications for mobility and combat modeling, *Photogrammetric Engineering and Remote Sensing*, 58, pp.1217-1221.

Niel, T.G.V. and McVicar, T.R., 2001. Remote Sensing of Rice-Based Irrigated Agriculture : A Review. Available on http://www.clw.csiro.au/publications/consultancy/2001/CRC-Rice-TRP11050101.pdf (Accessed 15 December 2009.)

Nuarsa, I.W. and Nishio, F., 2007. Relationships between rice growth parameters and remote sensing data. *Journal of Remote Sensing and Earth Sciences*, 4, pp.102-112.

Nuarsa, I.W., Kanno, S., Sugimori, Y. and Nishio, F., 2005. Spectral characterization of rice field using multi-temporal Landsat ETM+ data. *Journal of Remote Sensing and Earth Science*. 2, pp.65-71.

Okamoto, K. and Kawashima, H., 1999. Estimation of rice -planted area in the tropical zone using a combination of optical and microwave satellite sensor data. International *Journal of Remote Sensing*, 20, pp.1045-1048.

Pierce, F.J., Nowak, P. and Roberts, P.C., 1999. Aspects of Precision Agriculture, p.1-84. In *D.L. Sparks (ed.) Advances in Agronomy*, 67, Academic Press, San Diego, CA, USA.

Pons, X. and Solé-Sugrañes, L., 1994. A simple radiometric correction model to improve automatic mapping of vegetation from multispectral

satellite data. *Remote Sensing of Environment*, 48, pp.191-204.

Qin, Z. and Zhang, M., 2005. Detection of rice sheath blight for inseason disease management using multispectral remote sensing. *International Journal of Applied Earth Observation and Geoinformation*, 7, pp.115-128.

Ribbes, F. and Toan, L.T., 1999. Rice field mapping and monitoring using RADARSAT data. *International Journal of Remote Sensing*, 20, pp.745-765.

Shao, Y., Fan, X., Liu, H., Xiao, J., Ross, S., Brisco, B., Brown, R. and Staples, G., 2001. Rice monitoring and production estimation using multitemporal RADARSAT. *Remote Sensing of Environment*, 76, pp.310-325.

Thenkabail, P.S., Smith, R.B. and Pauw, D.E., 2000. Hyperspectral vegetation indices and their relationships with agricultural crop characteristics. *Remote Sensing of Environment*, 71, pp.158-182.

Thenkabail, P.S., Ward, A.D., Lyon, J.G. and Merry, C.J., 1994b. Thematic Mapper vegetation indices for determining soybean and corn growth parameters. *Photogrammetric Engineering and Remote Sensing*, 60, pp.437-442.

Tong, Q.T.Q., Pu, R., Guo, X., and Zhao, C., 2001. Spectroscopic determination of wheat water status using 1650-1850 nm spectral absorption features, *International Journal of Remote Sensing*, 22, pp.2329-2338.

Yang, C.-M. and Su, M.R., 2000. Analysis of spectr al character istics of r ice canopy under water deficiency : Monitor ing changes of spectral characteristics of dehydrating rice canopy. *Asian Conference on Remote Sensing*, 21, pp.13-18.

Yang, C.-M., and Chen, R.-K., 2004. Modeling rice growth using hyperspectral reflectance data. *Crop Science*, 44, pp.1283-1290.

Yang, C.-M., and Cheng, C.-H., 2001. Spectral characteristics of rice plants infested by brown planthopper. *Proceedings of the National Science Council*, 25, pp.180-186.

Yang, C.-M., Cheng, C.-H. and Chen, R.-K., 2007. Changes in spectral characteristics of rice canopy infested by leaf folder and brown planthopper. *Crop Science*, 47, pp.329-335.

Yang, C.-M., Liu, C.C., and Wang, Y.W., 2008. Using Formosat-2 Satellite Data to Estimate Leaf Area Index of Rice Crop. *Journal of Photogrammetry and Remote Sensing*, 13, pp.253-260.